

Anisotropic electrical transport in epitaxial $\text{La}_{2/3}\text{Ca}_{1/3}\text{MnO}_3$ thin films

V. S. Amaral

Departamento de Física, Universidade de Aveiro, 3810 Aveiro and IFIMUP, Universidade do Porto, 4150 Porto, Portugal

A. A. C. S. Lourenço

Departamento de Física, Universidade de Aveiro, 3810 Aveiro and INESC, 4150 Porto, Portugal

J. P. Araújo, A. M. Pereira, and J. B. Sousa

IFIMUP, Departamento de Física, Universidade do Porto, 4150 Porto, Portugal

P. B. Tavares

Departamento de Engenharia Cerâmica e do Vidro, Universidade de Aveiro, 3810 Aveiro and Secção de Química, Univ. de Trás-os-Montes e Alto Douro, 5000 Vila Real, Portugal

J. M. Vieira

Departamento de Engenharia Cerâmica e do Vidro, Universidade de Aveiro, 3810 Aveiro, Portugal

E. Alves, M. F. da Silva, and J. C. Soares

Instituto Tecnológico e Nuclear, E.N. 10, 2685 Sacavém, Portugal

Epitaxial thin films of $\text{La}_{0.62\pm 0.05}\text{Ca}_{0.33\pm 0.02}\text{MnO}_{3-\delta}$ were grown by laser ablation on SrTiO_3 . On (100) substrates the films grow with the larger c axis perpendicular to the plane. The films deposited on (110) SrTiO_3 grow with both the c (long) axis and a (or b , short) axis in the plane of the film. The electrical resistivity (ρ) and the magnetoresistance ($\Delta\rho/\rho$) show crystalline anisotropy. The resistivity ratio between the a and c axis is constant (0.8) from 10 K up to 120 K and decreases to 0.77 between 125 and 225 K, shows a small peak anomaly at T_c (257 K), and is almost constant in the paramagnetic phase. This temperature dependence is associated with anisotropic local lattice distortions. The magnetoresistance anisotropy ($\Delta\rho/\rho_{\parallel} - \Delta\rho/\rho_{\perp}$) with the applied field in the plane of the film, is small at low temperatures, peaks close to T_c , and is slightly larger for measurements along the a axis. The contributions of domain rotation and magnetocrystalline anisotropy to the anisotropic magnetoresistance associated with spin-orbit coupling are discussed. © 2000 American Institute of Physics. [S0021-8979(00)55108-1]

I. INTRODUCTION

The understanding of the mechanisms that affect the low field magnetic and electric properties of manganites, in particular thin films, is essential for its application in magnetoresistive devices. One of the mechanisms contributing to the low field magnetoresistance is the anisotropic magnetoresistance (AMR), which results from spin-orbit scattering, and depends on the square of the component of the magnetization transverse to the current direction. In this case, the contribution of magnetic domain configuration and magnetocrystalline anisotropy to the magnetoresistance is most relevant. On the other hand, contrary to the case of layered manganites, the crystallographic anisotropic properties of simple perovskite manganites have rarely been studied. We study the influence of crystallographic orientation on the resistivity and magnetoresistance of $\text{La}_{1-x}\text{Ca}_x\text{MnO}_3$ thin films. The importance of lattice distortions on the manganite properties has been established both theoretically and experimentally.¹ Our results suggest that the local lattice distortions of the Mn-O bonds also play a role in the anisotropic transport properties.

II. EXPERIMENTAL AND SAMPLE CHARACTERIZATION

Manganite thin films were deposited by laser ablation on SrTiO_3 (STO) substrates using bulk $\text{La}_{0.67}\text{Ca}_{0.33}\text{MnO}_3$ (LCMO) material ($T_c = 267$ K) as a target.² Epitaxial growth on (100) substrates will produce films with the c axis oriented perpendicular to the plane. On (110) STO substrates epitaxial growth is expected to keep the c axis in the plane, with one of the short axis along the normal.³ Here the LCMO orthorhombic structure is referred with the $Pbmm$ notation, with $a \approx b$ the short axis and c the larger axis. The films were structurally characterized by x-ray diffraction, texture, SEM and Rutherford backscattering spectrometry (RBS) with channeling. The crystalline quality of the films is excellent. The films deposited on (110) STO substrates present a RBS minimum yield of 10%–13% along the $\langle 110 \rangle$ substrate axis and 16%–20% along the $\langle 100 \rangle$ axis. The films deposited on (100) substrates have in general a slightly better crystalline quality, with minimum yields as low as 4.0% along the $\langle 100 \rangle$ substrate axis and 15% along the $\langle 110 \rangle$ axis. These values are among the lowest reported in the literature for manganite

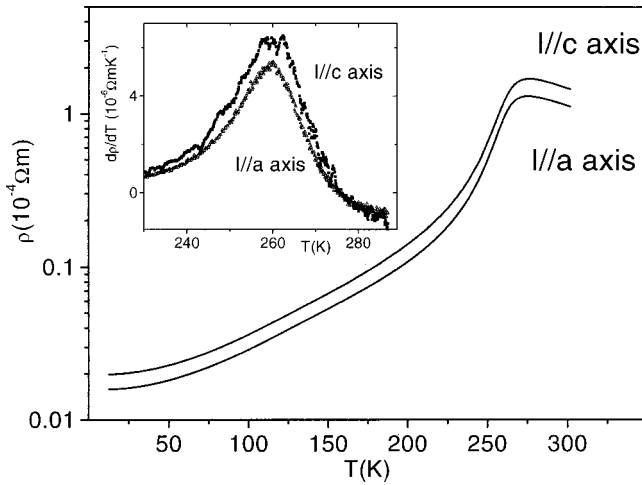


FIG. 1. Temperature dependence of the electrical resistivity with the current along the *a* or *c* manganite axis. The inset shows $d\rho/dT$ vs temperature.

thin films.⁴ The thickness and chemical composition of the films were determined using RBS data fitting. We find thicknesses between 1100 and 1700 Å and compositions $\text{La}_{0.62 \pm 0.05} \text{Ca}_{0.33 \pm 0.02} \text{MnO}_{3-\delta}$.

We present results on three of the samples; 100A and 110A, both deposited at 670 °C on (100) and (110) STO, respectively, and 110B, deposited on (110) STO at 700 °C. Texture measurements⁵ show that films on (100) substrates grow with the manganite *a* and *b* axis along the diagonals between [100] and [010] in plane axes of the substrate, while films on (110) substrates grow with the manganite *a* and *c* axes in plane, parallel to the $[1\bar{1}0]$ and the [001] axis of the substrate, respectively. Samples deposited on (100) and (110) STO under the same conditions present very similar characteristics,² showing that the films are thick enough to enable strain relaxation. For samples 100A and 110A, we find very close maxima of the temperature derivative of the electrical resistivity ($d\rho/dT$): 235 and 234 K, respectively. For sample 110B the $d\rho/dT$ maximum occurs at 260 K. The samples deposited on (110) STO allow the measurement of physical properties along two different crystallographic directions of the manganite, the short axis (*a/b*) and the long axis (*c*). We cut two oriented bar pieces, and measured the temperature dependence of the electrical resistivity with the electrical current (*I*) along the *a* or *c* axes. To reduce spurious effects and allow easier comparison of results, both bars were mounted with their axes parallel and measured simultaneously with the same current in series.

III. RESULTS AND DISCUSSION

The temperature dependence of the electrical resistivity along the two directions for sample 110B is displayed in Fig. 1. One finds that the electrical resistivity is indeed anisotropic, with the resistivity $\rho(I\parallel c)$ higher than $\rho(I\parallel a)$. As shown in Fig. 2, the ratio $\rho(I\parallel a)/\rho(I\parallel c)$ varies less than 4% in the whole temperature range. Up to about 150 K it is close to 0.80, and decreases to 0.76 at 225 K. At this temperature the resistivity anisotropy is maximum. A steep variation of the ratio occurs, with a sharp peak close to T_c (260 K). In the paramagnetic phase the ratio settles again at about 0.77. Un-

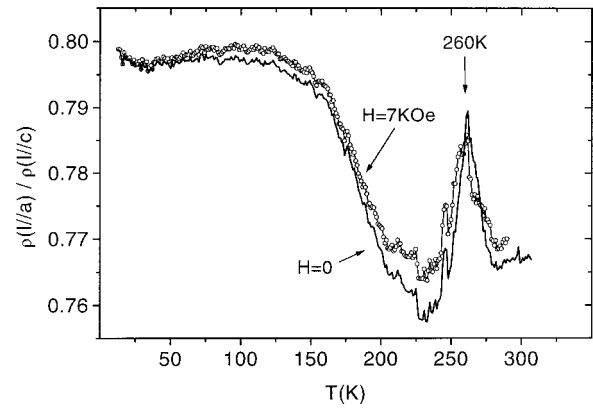


FIG. 2. Resistivity ratio $\rho(I\parallel a)/\rho(I\parallel c)$ with $H=0$ and 7 kOe. It is almost constant below about 150 K. Near 225 K the anisotropy of ρ is maximum.

der a magnetic field parallel to the axis $H=7$ kOe, the anisotropy variation is slightly reduced, and the peak close to T_c is broadened. Zeng and Wong⁶ studied the crystallographic anisotropy of LCMO thin films resistivity. They found that near and above T_c (200 K in their case) $\rho(I\parallel c)$ is higher than $\rho(I\parallel a)$. However, temperature dependence of the anisotropy was not the same and even changed sign below about 190 K. One should note that their study was made comparing two different films, which presented different T_c and resistivity peak temperatures. In our case, the $d\rho/dT$ peak temperatures are the same for the *a* and *c* bars (inset in Fig. 1). The sensitivity of electron scattering to short range effects may explain the temperature dependence of the resistivity crystalline anisotropy. Using Mn-edge EXAFS spectra, Lanzara *et al.*⁷ showed that LCMO (with $T_c=240$ K) presents two low temperature regimes, a truly ferromagnetic metal with homogeneously distributed large polarons only existing below a crossover temperature $T^* \approx 170$ K. Above T^* , in the so-called CMR phase, small and large polarons coexist, with an increasing fraction of longer Mn–O bonds (2.13 instead of 2.01 Å) along the Mn–O octahedra main axis. Above T_c , the small polarons still persist. The main characteristics of the temperature dependence of the resistivity ratio $\rho(I\parallel a)/\rho(I\parallel c)$ may be associated with this local structure change. An increase of Mn–O bonds along the *c*-axis would decrease the electron hopping probability, leading to an increase of the resistivity along the *c*-axis at T^* , consistent with our data. In layered manganites, Li *et al.* also recently considered the relevance of the local structure to the spin-independent conductance anisotropy.⁸

The magnetoresistance ($\Delta\rho/\rho$) of the samples was measured with the applied magnetic field in the plane, either parallel ($\Delta\rho/\rho_{\parallel}$) or transverse ($\Delta\rho/\rho_{\perp}$) to the current with magnetic field up to about 10 kOe, in both directions. The values found are of the usual order of magnitude for laser-ablated films near the optimally doped composition. In either configuration, $\Delta\rho/\rho$ presents a negative peak near T_c .² The magnetoresistance in the parallel configuration is in general larger (in absolute value) than in the perpendicular configuration, resulting in negative magnetoresistance anisotropy $\Delta\rho/\rho_{\parallel} - \Delta\rho/\rho_{\perp}$ (MRA). In ferromagnetic metals (Fe, Co, Ni), the MRA is directly related to the magnetization, and is al-

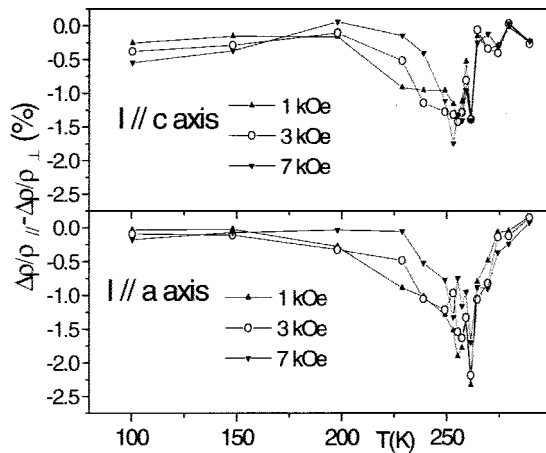


FIG. 3. Temperature dependence of the AMR, for $I//a$ and $I//c$, at constant magnetic field.

most constant in the ferromagnetic phase, decreasing to zero as the temperature is increased to T_c . In high quality magnetite films, MRA shows unusual temperature dependence, with a strong peak around T_c (MRA $\sim -1\%$ to -2%) and a much smaller limiting value at low temperatures (~ -0.2 to -0.4%).^{2,9} Figure 3 presents the temperature dependence of the MRA for sample 110B, with $I//a$ and $I//c$ in the intermediate and higher field range (1–7 kOe). At low temperatures, the MRA is low, around -0.5% and -0.2% for the c -axis and a -axis, respectively. Above T_c the MRA decreases to zero, and the a -axis MRA is more intense. In both these low and high temperature ranges the field dependence is weak. On the other hand, between about 200 K and T_c , the MRA presents a strong magnetic field dependence, which even becomes non monotonic. In this interval, one finds that resistivity jumps occur at the coercive fields ($H_c \sim 80$ kOe) if the magnetic field is applied in the a/b axis, on both 100 and 110 samples.^{2,5} Such a feature is associated with a rapid magnetization reversal through the growth of aligned magnetic domains at the expense of antiparallel or transverse domains.¹⁰ To further characterize the nature of the MRA we studied the dependence of the electrical resistivity on the angle θ between the electric current and the in-plane applied magnetic field, $\Delta\rho/\rho(\theta) = (\rho(\theta)/\rho(0) - 1)$. The mechanism of anisotropic magnetoresistance (AMR), that results from local spin-orbit scattering of conduction electrons leads to a direct dependence on the square of the component of the magnetization transverse to the current direction,¹¹ $\rho(\varphi) = \rho_0 + \Delta\rho \sin^2 \varphi$, where φ is the angle between the magnetization and the electric current. In a saturated ferromagnet, with a magnetic field (\mathbf{H}) large enough to keep the magnetization (\mathbf{M}) aligned with it ($\varphi = \theta$), the resistivity should have the same dependence on the angle θ as the magnetic field is rotated in the plane of the sample. Figure 4 shows the results for sample 110A with the current along the c axis ($\theta = 0$) at 100 K and 200 K. At low temperatures and sufficiently high magnetic fields ($H = 7$ kOe) one finds the characteristic AMR angular dependence. At lower fields ($H = 1$ kOe), however, the angular dependence is different, in-

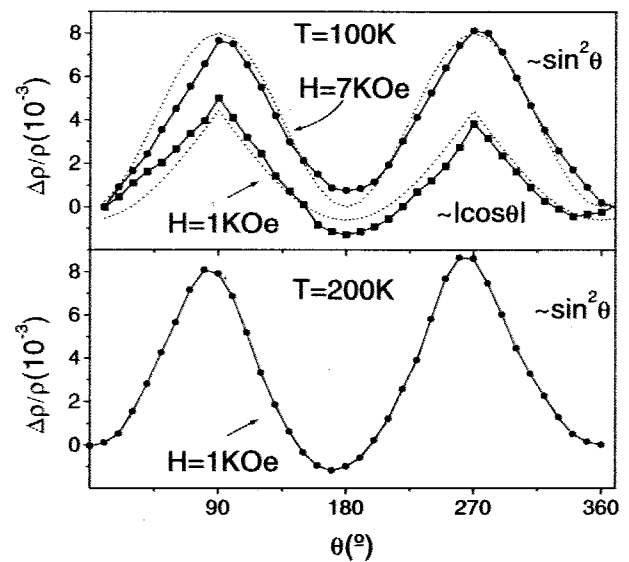


FIG. 4. Angular dependence of the resistivity as the magnetic field is rotated in the plane of the sample (θ) for current along the c axis ($\theta = 0$). Dashed lines indicate the AMR ($\sin^2 \theta$) and CMR ($|\cos \theta|$) dependencies.

dicating that \mathbf{M} is not aligned with \mathbf{H} . At higher temperatures, the $\sin^2 \theta$ dependence is observed even at 1 kOe. These results can be interpreted using a phenomenological model introduced by O'Donnell *et al.*¹⁰ considering the magnetization dependence of both the colossal magnetoresistance (CMR) and AMR effects. $\rho(H, \theta) = \rho_0(1 - A|H \cos(\theta - \varphi)|) \times (1 + B \sin^2 \varphi)$. The linear magnetic field dependence of the CMR term is appropriate only at low temperatures. The analysis of magnetization configurations with adequate symmetry anisotropy energy contributions reveals that at sufficiently low fields \mathbf{M} will not deviate much from an easy axis ($\varphi \ll 1$) and therefore the CMR term will dominate, with a $|\cos \theta|$ dependence. At high enough fields, $\varphi = \theta$ and the AMR dependence is recovered. The observation of the AMR dependence for $H = 1$ kOe at 200 K is consistent with a decrease of the anisotropy energy with increasing temperatures. This competition of effects is also observed in a recent study on layered magnetites.¹²

ACKNOWLEDGMENTS

J.P.A. and A.M.P. acknowledge scholarships from JNICT/FCT. The work is partially supported by JNICT/FCT under the Contracts Nos. PBIC/C/CTM/1967/95. PRAXIS/3/3.1/Fis/21/94, and PRAXIS/P/CTM/13142/98.

- ¹J. M. D. Coey, M. Viret, and S. von Molnár, *Adv. Phys.* **48**, 167 (1999).
- ²A. A. C. S. Lourenço *et al.*, *J. Magn. Magn. Mater.* **196–197**, 495 (1999).
- ³P. R. Broussard *et al.*, *Appl. Surf. Sci.* **115**, 80 (1997).
- ⁴V. A. Vas'ko *et al.*, *Appl. Phys. Lett.* **68**, 2571 (1996); G. C. Xiong *et al.*, *ibid.* **66**, 1247 (1995).
- ⁵V. S. Amaral *et al.*, *J. Magn. Magn. Mater.* (in press).
- ⁶X. T. Zeng and H. K. Wong, *Appl. Phys. Lett.* **72**, 741 (1998).
- ⁷A. Lanzara *et al.*, *Phys. Rev. Lett.* **81**, 878 (1998).
- ⁸Q. A. Li *et al.*, *Phys. Rev. B* **59**, 9357 (1999).
- ⁹M. Ziese and S. P. Sena, *J. Phys.: Condens. Matter* **10**, 2727 (1998).
- ¹⁰J. O'Donnell *et al.*, *Phys. Rev. B* **55**, 5873 (1997).
- ¹¹E. Dan Dahlberg, K. Riggs, and G. A. Prinz, *J. Appl. Phys.* **63**, 4270 (1988), and references therein.
- ¹²T. Okuda *et al.*, *Phys. Rev. B* **60**, 3370 (1999).